




Original Research

COL11A1 Inhibits Ferroptosis in Pancreatic Cancer by Regulating AKT/Beclin 1 Dependent Autophagy

Hui Wang¹, Shuang Zhi¹, Zibo Yang¹, Na Gu¹, Linlin Dai¹, Jun Cai¹,
Juan Wang², Dongdong Li^{1,*}¹Medicinal Synthesis Research Laboratory, Tianjin Institute of Medical & Pharmaceutical Sciences, 300020 Tianjin, China²Department of Genetics, Tianjin Medical University, 300070 Tianjin, China*Correspondence: lidongdong2010@163.com (Dongdong Li)

Academic Editors: Flavia Biamonte and Graham Pawelec

Submitted: 17 December 2025 Revised: 20 January 2026 Accepted: 12 February 2026 Published: 19 March 2026

Abstract

Background: Collagen type XI alpha 1 (COL11A1) is overexpressed in pancreatic cancer and is often associated with poor survival, chemoresistance, and tumor recurrence. However, the role of COL11A1 in pancreatic cancer remains poorly understood. **Methods:** We explored the correlation between COL11A1 and overall survival in pancreatic cancer patients using Kaplan-Meier survival analysis and validated COL11A1's regulatory role in the viability of pancreatic cancer cell line PANC-1 using Cell Counting Kit-8 and colony formation assays. To clarify the underlying mechanisms, we further examined COL11A1's modulation of ferroptosis and autophagy in PANC-1 cells by western blot, reverse transcription quantitative polymerase chain reaction (RT-qPCR), and immunofluorescence assays. Moreover, autophagy agonist rapamycin, inhibitor 3-methyladenine (3-MA), and AKT/Beclin 1 pathway inhibitors were employed to dissect the regulatory crosstalk between COL11A1, autophagy, and ferroptosis. **Results:** COL11A1 expression was negatively correlated with pancreatic cancer patients' survival rate. Its overexpression significantly enhanced the viability and clonogenic capacity of erastin- and rapamycin-treated PANC-1 cells. Our data showed that COL11A1 reduced intracellular iron levels, suppressed reactive oxygen species accumulation, downregulated malondialdehyde and microtubule-associated protein 1 light chain 3-II/I (LC3II/I) expression, while increasing glutathione (GSH), ferritin heavy chain 1 (FTH1) and solute carrier family 7 member 11 (SLC7A11) levels. Furthermore, COL11A1-mediated ferroptosis inhibition was attenuated by the autophagy agonist Rapamycin but enhanced by the inhibitor 3-MA. Notably, COL11A1 promoted AKT and Beclin 1 phosphorylation, and blocking the AKT/Beclin 1 pathway abrogated its ability to suppress autophagy and ferroptosis in pancreatic cancer cells. **Conclusions:** The study demonstrated that COL11A1 exerts its oncogenic effects by suppressing autophagy via the AKT/Beclin 1 pathway, consequently inhibiting ferroptosis in pancreatic cancer cells. These findings reveal a novel molecular mechanism through which COL11A1 promotes tumor progression and provide a potential therapeutic target for pancreatic cancer treatment.

Keywords: collagen type XI alpha 1 chain; ferroptosis; autophagy; AKT/Beclin 1 pathway; pancreatic ductal carcinoma

1. Introduction

Pancreatic cancer is a highly aggressive malignancy with a dismal prognosis and limited therapeutic advancements. Pancreatic ductal adenocarcinoma (PDAC) accounts for 85–90% of cases—it arises from pancreatic ductal epithelial cells, characterized by dense stroma, high metastatic potential, and inherent therapeutic resistance. GLOBOCAN 2020 reports ~496,000 new cases and 466,000 deaths annually globally. Set to be the US's second leading cancer killer by 2030 (~64,000 new cases in 2024), China records ~128,000 new cases and 121,000 deaths yearly. With >80% of patients diagnosed at advanced stages, the global 5-year overall survival rate is merely 10–12%, and post-resection recurrence exceeds 70% [1,2]. This highlights the urgent need to elucidate PDAC's pathogenic mechanisms for novel biomarkers and therapies.

Collagen type XI alpha 1 (COL11A1) belongs to the collagen family. While it plays a role in skeletal devel-

opment [3], it is also significantly associated with tumor metastasis, treatment resistance, and poor prognosis in various solid tumors such as colorectal, breast, and ovarian cancers [4,5]. As a key component of the extracellular matrix, COL11A1 serves as a predictive marker for aggressive immune infiltration in pancreatic cancer and regulates signaling pathways involved in cell survival and stress responses [6]. Among these, autophagy and ferroptosis have garnered widespread attention due to their dual roles in tumor progression and treatment resistance. Investigating whether COL11A1 influences PDAC development by regulating autophagy-ferroptosis crosstalk may provide novel insights into its oncogenic mechanisms.

Studies have shown that members of the collagen family, such as Collagen I and Collagen VI, are closely associated with cellular autophagy [7,8], suggesting that Collagen XI may also be involved in this process. Autophagy and regulated cell death, such as ferroptosis, can determine cellular fate by activating interconnected signaling cascades



and regulating gene expression profiles [9]. Autophagy, also known as “self-eating”, is a group of mechanisms that transport proteins and organelles to the lysosome or vacuole for destruction [10]. It is essential for tissue and cellular homeostasis, and dysregulation of autophagy is associated with numerous pathologies, including neurodegenerative diseases, cancer, and Crohn’s disease [11]. An important autophagy protein, Beclin 1, can form different complexes that are involved in autophagosome initiation and autolysosome maturation. Beclin 1-dependent autophagy protects multiple organs, such as the heart, lung and liver, during the pathogenesis of sepsis [12]. Under specific conditions, autophagy plays a key role in driving ferroptosis [13,14]. Autophagy-mediated ferritin deposition may influence the efficacy of anticancer therapy, the progression of inflammatory responses, and the occurrence and development of tissue fibrosis [9,15].

Ferroptosis, a newly identified iron-dependent cell death modality, is characterized by intracellular iron accumulation, lipid peroxidation product (malondialdehyde [MDA]) accumulation, glutathione depletion, and reduced glutathione peroxidase 4 (GPX4) activity, ultimately causing lipid membrane damage and perforation [16–18]. Ferroptosis can be induced by either the intrinsic or extrinsic mechanism. The intrinsic pathway is predominantly activated by suppressing the expression or function of intracellular antioxidant enzymes, such as GPX4. In contrast, the extrinsic pathway is initiated by modulating transporters, including inhibiting the amino acid antiporter system xc or activating the iron transporters transferrin and lactoferrin [19]. Mitochondria have a dual function in this process: they produce reactive oxygen species (ROS) that increase oxidative stress and release stored iron, which enhances Fenton reactions that intensify lipid peroxidation [20]. Accumulating evidence supports ferroptosis modulation (induction or inhibition) as a promising cancer therapeutic strategy, enhancing radiotherapy [21] and chemotherapy efficacy [22,23]. Characterized by hyperactive mitochondrial fission and inherently strained redox balance, inducing ferroptosis is a promising therapeutic strategy for PDAC [24], thus making elucidation of ferroptosis regulatory mechanisms crucial for developing effective therapies.

Activation of AMP-activated protein kinase (AMPK) and AKT is closely associated with ROS production [25], and both play important roles in autophagy and lipid metabolism [26–28]. The ROS/AMPK/mTOR pathway can induce autophagy, while ROS inhibits AKT activity through dephosphorylation of AKT at Ser-473 [29]. Beclin 1 is a key autophagic protein and also a molecular target of AKT. AKT-mediated phosphorylation of Beclin 1 plays a role in autophagy inhibition [30]. Thus, we speculated that COL11A1 regulates autophagy through the AKT/Beclin 1 signaling pathway.

In the present study, we investigated the biological role and underlying molecular mechanism of COL11A1

Table 1. Sequences of siRNAs.

Gene	siRNA sequences (5' to 3')
<i>siBeclin 1-1</i>	5'-GGAGTCTCT GACAGACAAA-3'
<i>siBeclin 1-2</i>	5'-GGAGCCAUUUAUUGAACUTT-3'

in autophagy and ferroptosis in PDAC. We demonstrate that COL11A1 inhibits ferroptosis in PDAC by suppressing AKT/Beclin 1-dependent autophagy.

2. Materials and Methods

2.1 Cell Culture and Reagents

The PANC-1 PDAC cell line was purchased from Procell Life Science & Technology Co., Ltd. (Wuhan, China). The cell lines used in this study were authenticated by short tandem repeat (STR) profiling and tested negative for mycoplasma. Small interfering RNAs (siRNAs) against Beclin 1 were synthesized by GenePharma (Shanghai, China), the sequences are shown in Table 1. We obtained the pCMV3-COL11A1 plasmid from Sino Biological (Cat.No: HG18256-UT; Beijing, China). LY294002 (a PI3K inhibitor) and erastin (a ferroptosis promoter) were obtained from Beyotime (Shanghai, China). Rapamycin (RAPA, autophagy promoter) was obtained from MedChemExpress (Cat.No: HY-10219, Monmouth Junction, NJ, USA).

2.2 Cell Counting Kit-8 Assay

Cells were seeded in 96-well plates before receiving different treatments. Cell viability was assessed at 24, 48, and 72 h intervals using a Cell Counting Kit-8 (CCK-8) assay in accordance with the manufacturer’s instructions. After the indicated treatments, cells seeded in a 96-well plate were incubated with 10 µL of CCK-8 reagent (Cat.No: CK04, Dojindo, Kumamoto, Japan) per 100 µL of culture medium for 1–4 h at 37 °C in a humidified incubator. The absorbance at 450 nm was then measured.

2.3 Western Blotting

All cellular extracts were obtained by lysis in radioimmunoprecipitation assay (RIPA) buffer (Solarbio, Beijing, China). Protein concentrations were determined using a bicinchoninic acid (BCA) kit (ThermoFisher Scientific, Waltham, MA, USA). Subsequently, 30 µg protein per sample was separated by 10% sodium dodecyl sulfate polyacrylamide gel electrophoresis (SDS-PAGE) and electrotransferred onto a polyvinylidene difluoride (PVDF) membrane. After blocking with 5% non-fat milk, the membrane was incubated with primary antibodies at 4 °C overnight, followed by incubation with the corresponding secondary antibody for 1 h. Finally, protein bands were detected using ECL reagent (Millipore, Burlington, MA, USA) and visualized using the LAS500 gel imaging system (GE, Massachusetts, NY, USA). The antibodies used are listed in Table 2.

Table 2. Antibodies used for western blotting analysis.

Name	Company	Catalog number	Antibody concentration
GPX4	Cell Signaling Technology, USA	#52455S	1:1000
NCOA4	Cell Signaling Technology, USA	#66849S	1:1000
FTH1	Cell Signaling Technology, USA	#3998S	1:1000
p62	Cell Signaling Technology, USA	#5114S	1:1000
AKT	Cell Signaling Technology, USA	#9272S	1:1000
p-AKT ^{Ser473}	Cell Signaling Technology, USA	#4060S	1:2000
LC3	Cell Signaling Technology, USA	#12741S	1:1000
mTOR	Cell Signaling Technology, USA	#2972S	1:1000
p-mTOR	Cell Signaling Technology, USA	#5536T	1:1000
Beclin 1	Cell Signaling Technology, USA	#3738S	1:1000
p-Beclin 1	Cell Signaling Technology, USA	#14717S	1:1000
β -actin	Sungene Biotech, China	#KM9001	1:5000
Goat anti-rabbit IgG	ZSGB-Bio, China	#ZB-2301	1:5000
Goat anti-mouse IgG	ZSGB-Bio, China	#ZB-2305	1:5000

Table 3. Primer sequences used for real-time polymerase chain reaction (PCR) analysis.

Gene	Primers sequences (5' - 3')
<i>GAPDH</i>	F: AGCCACATCGCTCAGACAC R: GCCCAATACGACCAAATCC
<i>FTH1</i>	F: TGAAGCTGCAGAACCAACGAGG R: GCACACTCCATTGCATTGAGCC
<i>GPX4</i>	F: ACAAGAACGGCTGCGTGGTGAA R: GCCACACACTTGTGGAGCTAGA
<i>SLC7A11</i>	F: TCCTGCTTTGGCTCCATGAACG R: AGAGGAGTGTGCTTGCGGACAT
<i>LC3</i>	F: GATGTCCGACTTATTCGAGAGC R: TTGAGCTGTAAGCGCCTTCTA
<i>P62</i>	F: AGAACGTTGGGGAGAGTGTG R: GCGATCTTCTCATCTGCTC

2.4 Real-Time PCR

Total RNA was extracted using the Total RNA Extraction Kit (Promega, Madison, WI, USA) according to the manufacturer's instructions. Then, it was reverse-transcribed into cDNA using a HiFiScript first-strand cDNA synthesis kit (CW BIO, Beijing, China). Real-time PCR was performed using ChamQ™ Universal SYBR qPCR Master Mix (CW BIO, Beijing, China) and detected using an Applied Biosystems 7500 Fast Dx Real-time PCR Instrument (Thermo Fisher Scientific, Rockford, IL, USA). The relative mRNA expression was calculated using the $2^{-\Delta\Delta C_t}$ method. The primer sequences used in this study are listed in Table 3.

2.5 Immunofluorescence Assay

PANC-1 cells were seeded onto coverslips placed in a 24-well plate. After treatment, the cells on the coverslips were fixed and permeabilized followed by blocking in 10% goat serum for 1 h. Then the coverslips were incubated with

LC3 antibody (1:200) at 4 °C overnight, followed by incubation with fluorescently labeled secondary antibody at room temperature for 1 h. Nuclei were stained with DAPI. After washing three times with phosphate buffered saline with Tween-20 (PBST), images were captured using a fluorescence microscope.

2.6 Determination of Iron Content

FeRhoNox-1 (Cat. No.: MX4558; MaokangBio, Shanghai, China) was used to detect intracellular iron content. Cells were seeded in 24-well plates, cultured overnight, and then treated with rhCOL11A1/pCMV3-COL11A1 and erastin for 48 h. After collection, cells were washed twice with preheated PBS, incubated with 5 μ M FeRhoNox-1 at 37 °C for 60 min in the dark, and then washed three times with preheated PBS. Nuclei were stained with DAPI, followed by three additional PBS washes, and images were acquired by fluorescence microscopy. Differences in average fluorescence intensity reflect varying intracellular iron levels.

2.7 Lipid Peroxidation Assay

BODIPY™ 581/591 C11 (Cat.No.: D3861; Thermo Fisher Scientific, USA) was used to detect intracellular lipid peroxidation. Cells were seeded in 24-well plates, cultured overnight, and treated with rhCOL11A1/pCMV3-COL11A1 and erastin for 48 h. After collection, cells were washed twice with preheated PBS, incubated with 10 μ M BODIPY™ 581/591 C11 at 37 °C for 30–60 min in the dark, and washed three times with preheated PBS. Nuclei were stained with DAPI, followed by three additional PBS washes. Images were captured via fluorescence microscopy, and differences in average fluorescence intensity reflect varying levels of lipid peroxidation.

2.8 Mitochondrial Membrane Potential Assay

PANC-1 cells were seeded onto coverslips that had been previously placed in a 24-well plate. Following treatment, cells were washed and incubated with JC-1 working solution at 37 °C for 30 min. After washing three times with pre-warmed buffer to eliminate unbound dye, fluorescence detection was performed immediately, with red fluorescence indicating aggregated JC-1 and green fluorescence representing monomeric JC-1. A Mitochondrial Membrane Potential Detection Kit (JC-1) was purchased from Beyotime (No: C2006).

2.9 GSH Assay

Cells were seeded into 6-well plates and cultured overnight. After different treatments, each sample was collected and washed twice with PBS. The cell precipitate was resuspended in a reagent with a volume three times that of the precipitate, and the resulting suspension was lysed by ultrasound (200 W, ultrasound 3 s, interval 10 s, repeated 30 times) and centrifuged at 4 °C for 10 min. Then the samples were analyzed using a glutathione (GSH) content detection kit (No: BC1175; Solarbio).

2.10 MDA Assay

After treatment, the cells were collected and incubated in lysis buffer for 2 h at 4 °C. Then the mixture was centrifuged for 10 min to obtain the supernatant for subsequent analyses. Cell samples were lysed in ice-cold RIPA buffer containing protease inhibitors. After centrifugation, the supernatant was collected. For the reaction, 100 μ L of supernatant was mixed with 200 μ L of 8.1% SDS, 750 μ L of thiobarbituric acid (TBA) working solution (0.8% thiobarbituric acid in 20% acetic acid, pH 3.5), and 750 μ L of 20% acetic acid. The mixture was vortexed, incubated at 95 °C for 60 minutes, and then cooled on ice. Absorbance was measured at 532 nm in a 96-well plate. MDA concentration was quantified against a standard curve prepared using tetraethoxypropane and normalized to total protein content determined by the BCA assay. Lipid peroxidation was quantified using an MDA assay kit (No: S0131S; Beyotime).

2.11 ROS Assay

Cells were seeded in a 24-well plate and treated for 48 h. After discarding the culture medium, the samples were processed for analysis according to the manufacturer's protocol. Intracellular ROS levels were measured via immunofluorescence assays using an ROS assay kit (No: S0033s; Beyotime).

2.12 Colony Formation Assay

PANC-1 cells were seeded into 6-well plates at a density of 3×10^3 cells per well and cultured under standard conditions (37 °C, 5% CO₂) for 7–14 days while receiving separate treatments. The cells were fixed for 15 min,

air-dried, and stained with Giemsa stain for 20 min before being washed with PBS. The colony formation rate was calculated using the following formula: (number of colonies formed \div number of inoculated cells) \times 100%.

2.13 In Vivo Antitumor Activity

The nude mice (BALB/c-nu, weighing 13–16 g) were purchased from Beijing Vital River Laboratory Animal Technology Co., Ltd. To establish subcutaneous xenograft models, 20 nude mice were randomly divided into two groups. The control group (n = 5) received subcutaneous injection of PANC-1 cells at a dose of 5×10^6 cells per mouse, while the experimental group (n = 15) was subcutaneously injected with COL11A1-overexpressing PANC-1 cells at the same dosage (5×10^6 cells/mouse) to evaluate the effect of COL11A1 overexpression on tumor growth.

Treatment began when the implanted tumors reached a volume of approximately 50 mm³, and the mice were divided into four groups. The control group was administered with physiological saline via intraperitoneal injection. A total of 15 nude mice inoculated with the COL11A1-overexpressing cell line were equally divided into three subgroups, with the following treatment regimens applied via intraperitoneal injection respectively: The first subgroup received physiological saline; the second subgroup was treated with erastin at a dose of 30 mg/kg, 2–3 times per week; the third subgroup was given RAPA at a dose of 4 mg/kg, 2–3 times per week. All experimental animals were humanely euthanized by cervical dislocation in accordance with institutional animal care and use guidelines.

Tumor volumes were calculated from formula: $TV = 1/2 \times a \times b^2$, where “a” is the tumor length and “b” is the width and both “a” and “b” were measured by a vernier caliper. Post treatment mice were sacrificed on day 22, and tumors were removed for further analysis.

The experimental procedures and the animal use and care protocols were approved by the Committee on Ethics of Tianjin Institute of Medical and Pharmaceutical Sciences.

2.14 Statistical Analysis

All statistical analyses and graphical visualizations were conducted with GraphPad Prism v 6.0.1 for Windows (GraphPad Software, Boston, MA, USA). Data from three independent experiments are presented as the mean \pm standard deviation (SD). To compare the experimental groups with the control group, Student's *t*-test and analysis of variance were employed. $p < 0.05$ was considered statistically significant.

3. Results

3.1 COL11A1 Inhibited Pancreatic Cancer Cells Death by Regulating Autophagy and Ferroptosis

Kaplan Meier survival analysis showed that the expression of COL11A1 was negatively correlated with the

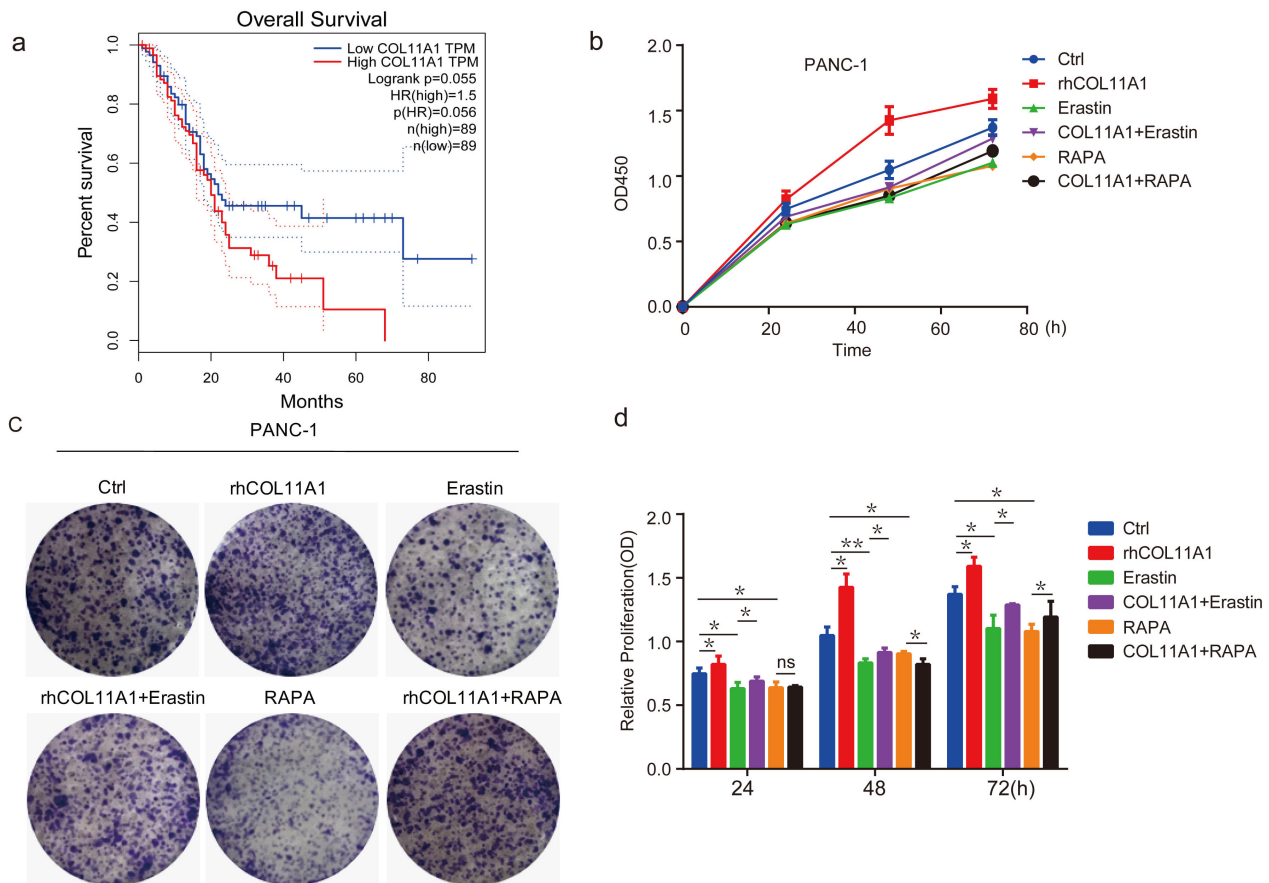


Fig. 1. COL11A1 inhibited PANC-1 cell death by regulating autophagy and ferroptosis. (a) Kaplan–Meier Analysis of the correlation between COL11A1 expression and survival outcomes in patients with pancreatic cancer. (b) CCK-8 assay was used to detect cell viability under different treatments with COL11A1, erastin (10 μ M), or RAPA (100 nM). (c) Colony formation assay was performed in PANC-1 cells with different treatments. (d) CCK-8 assay was performed, and the results are presented as a bar chart showing the viability of PANC-1 cells among different treatment groups. Data are expressed as the mean \pm SD from three independent experiments with triplicate wells per group. $n = 3$, $*p < 0.05$; $**p < 0.01$; ns, not significant. COL11A1, collagen type XI alpha 1; CCK-8, Cell Counting Kit 8; RAPA, rapamycin.

survival rate of patients with pancreatic cancer (Fig. 1a). The results of the CCK-8 assay showed that COL11A1 inhibited PANC-1 cell death, and erastin and RAPA weakened the effects of COL11A1 on PANC-1 cells (Fig. 1b,d). Moreover, cloning experiments confirmed that COL11A1 inhibits PANC-1 cell death, and that its inhibitory mechanism may be linked to autophagy and ferroptosis (Fig. 1c). These results indicate that COL11A1 inhibits pancreatic cancer cell death by regulating autophagy and ferroptosis.

3.2 COL11A1 Suppressed Ferroptosis in Pancreatic Cancer Cells

To further validate that COL11A1 participates in regulating ferroptosis in pancreatic cancer cells, we performed western blotting to assess the expression of key ferroptosis-related proteins under COL11A1 modulation. The data demonstrated that COL11A1 significantly enhanced the protein and mRNA expression levels of GPX4, ferritin

heavy chain 1 (FTH1), and solute carrier family 7 member 11 (SLC7A11), supporting its regulatory role in the ferroptosis process (Fig. 2a and Fig. 3c). Iron ion content and lipid peroxidation are key indicators of ferroptosis. Specifically, MDA is an end-product marker of lipid peroxidation, whereas GSH is a key antioxidant molecule inhibiting lipid peroxidation. In PANC-1 cells treated with COL11A1, MDA levels were decreased whereas GSH levels were increased (Fig. 2b). Next, the BODIPY 581/591 C11 probe was used to detect lipid peroxidation levels in erastin-pretreated PANC-1 cells. Cells in the COL11A1 treatment groups exhibited a distinct fluorescence shift from green to red, indicating a significant reduction in lipid peroxidation levels (Fig. 2d). Given that lipid peroxidation primarily occurs in mitochondria, we used the JC-1 probe to detect mitochondrial membrane potential (MMP) changes in PANC-1 cells. The COL11A1 treatment group showed predominant red fluorescent J-aggregates, indicating that COL11A1 attenuated erastin-induced MMP disruption in

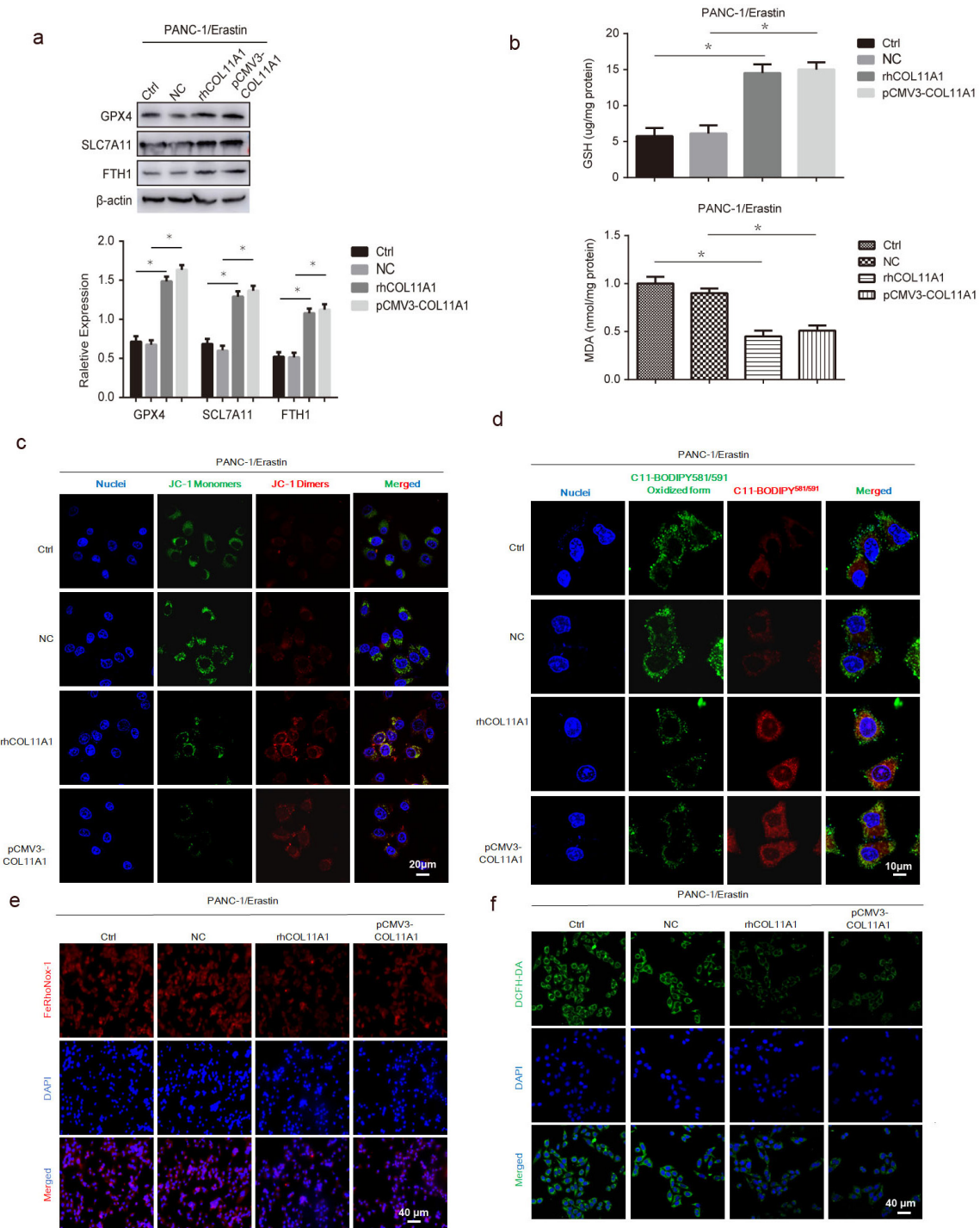


Fig. 2. COL11A1 inhibited ferroptosis in pancreatic cancer cells. (a) Western blotting was used to detect the protein expression levels of GPX4, SLC7A11, and FTH1 under treatment with erastin (10 μM) and transfected pCMV3-COL11A1, or rhCOL11A1. (b) GSH/MDA kit was used to detect the expression level of GSH/MDA under treatment with erastin (10 μM) and transfected pCMV3-COL11A1 or rhCOL11A1. (c) The JC-1 probe was employed to assess the impact of COL11A1 on MMP. Scale bar: 20 μm. (d) Representative images of C11-BODIPY^{581/591} stained COL11A1 overexpressed PANC-1 cells treated with 10 μM erastin for 12 h. A shift in the green-to-red ratio indicates lipid oxidation. Scale bar: 10 μm. (e) The FeRhoNox-1 probe was employed to determine the iron ion concentration under different treatment conditions. Scale bar: 40 μm. (f) Immunofluorescence was used to detect the expression of ROS by adding DCFH-DA under different treatment. Scale bar: 40 μm. n = 3, *p < 0.05. GPX4, glutathione peroxidase 4; SLC7A11, solute carrier family 7 member 11; FTH1, ferritin heavy chain 1; MDA, malondialdehyde; MMP, mitochondrial membrane potential; ROS, reactive oxygen species; GSH, glutathione; JC-1, 5,5',6,6'-tetrachloro-1,1',3,3'-tetraethylbenzimidazolcarbocyanine iodide; DCFH-DA, 2',7'-dichlorodihydrofluorescein diacetate.

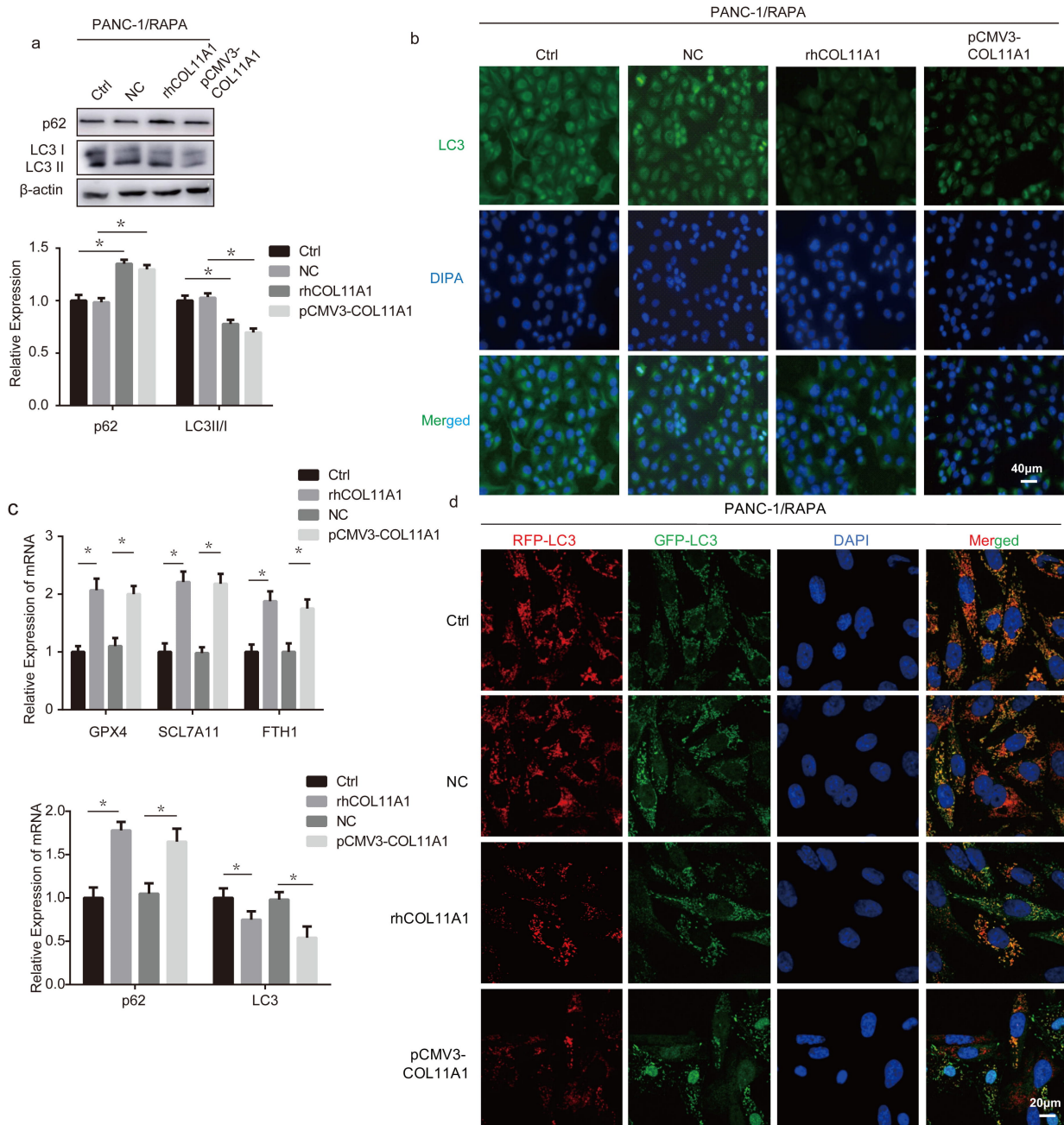


Fig. 3. COL11A1 inhibited autophagy in pancreatic cancer cells. (a) Western blotting was used to detect the expression levels of LC3 and p62 under treatment with RAPA (100 nM) and transfected pCMV3-COL11A1 or rhCOL11A1. (b) Immunofluorescence was used to detect the expression of LC3 under treatment with RAPA (100 nM) and transfected pCMV3-COL11A1 or rhCOL11A1. Scale bar: 40 μ m. (c) RT-PCR was used to detect the mRNA expression level of GPX4, SCL7A11, FTH1, p62 and LC3 under treatment with erastin (10 μ M) or RAPA (100 nM) and transfected pCMV3-COL11A1, or rhCOL11A1. (d) rhCOL11A1 or pCMV3-COL11A1 plasmid was co-transfected with CMV-TurboRFP-EGFP-LC3-PGK-Puro plasmid into PANC-1 cells, followed by treatment with 100 nM RAPA. The fluorescence spots were detected. Scale bar: 20 μ m. $n = 3$, $*p < 0.05$. LC3, microtubule-associated proteins 1A/1B light chain 3.

PANC-1 cells (Fig. 2c). Finally, we performed immunofluorescence staining to assess the intracellular levels of iron and ROS—two core mediators of ferroptosis. The results showed that compared with the control group, iron and ROS levels were significantly downregulated in PANC-1 cells treated with COL11A1 (Fig. 2e,f). Furthermore, no sig-

nificant differences were observed in the key ferroptosis-related indicators between the rhCOL11A1 treatment group and the pCMV3-COL11A1-transfected group. Taken together, these results demonstrated that COL11A1 exerts an inhibitory effect on ferroptosis in PANC-1 cells.

3.3 COL11A1 Exerts Autophagy-Inhibitory Effect on Pancreatic Cancer Cells

To further confirm that COL11A1 is involved in regulating autophagy in pancreatic cancer cells, we analyzed its effect on the expression of autophagy-related proteins. Western blotting analysis showed that COL11A1 reduced the conversion of LC3I to LC3II and increased p62 expression in PANC-1 cells (Fig. 3a). Immunofluorescence staining revealed decreased average fluorescence intensity of LC3 in COL11A1-treated PANC-1 cells (Fig. 3b). RT-PCR results showed that COL11A1 reduced the mRNA expression of LC3 and increased p62 mRNA expression in PANC-1 cells (Fig. 3c). Indeed, PANC-1 cells were transfected with CMV-TurboRFP-EGFP-LC3-PGK-Puro plasmid to detect autophagy flux, and the results showed that in COL11A1-overexpressing PANC-1 cells, there was a significant reduction in the number of both yellow and red-only puncta compared with wild-type cells. To monitor autophagic flux, PANC-1 cells were transfected with the CMV-TurboRFP-EGFP-LC3-PGK-Puro plasmid. The results showed that both the pCMV3-COL11A1 plasmid and rhCOL11A1 significantly blocked autophagic flux (Fig. 3d). Collectively, these results indicated that COL11A1 inhibits autophagy in PANC-1 cells.

3.4 COL11A1 Regulates the Ferroptosis Process of Pancreatic Cancer Cells Through Autophagy

Literature reports indicate that autophagy is involved in regulating the ferroptosis process of cells [9,14]. To further explore the molecular mechanism by which COL11A1 regulates autophagy and ferroptosis in PANC-1 cells, we simultaneously co-treated the cells with 3-methyladenine (3-MA) (an autophagy inhibitor), RAPA (an autophagy inducer), and pCMV3-COL11A1. Changes in ferroptosis-related proteins were detected using western blotting and fluorescence assays. The results showed that 3-MA upregulated the expression of GPX4, FTH1, and SLC7A11, thereby enhancing the inhibitory effect of COL11A1 on ferroptosis in PANC-1 cells. By contrast, RAPA exerted the opposite effect, inhibiting the regulatory role of COL11A1 in ferroptosis (Fig. 4a). In addition, immunofluorescence results demonstrated that the levels of ROS and iron content were increased in the COL11A1+RAPA combined treatment group compared with the COL11A1 monotherapy group, whereas these levels were decreased in the COL11A1+3-MA combined treatment group (Fig. 4b,c). We further examined the effects of RAPA and 3-MA on COL11A1-induced changes in GSH and MDA levels. The results showed that RAPA attenuated the regulatory effect of COL11A1 on GSH and MDA levels, whereas 3-MA enhanced this regulatory effect of COL11A1 (Fig. 4d). Collectively, these findings demonstrated that autophagy inhibition partially alleviated ferroptosis in the context of COL11A1 exposure. In summary, COL11A1 diminishes cellular sensitivity to ferroptosis by inhibiting autophagy.

3.5 COL11A1 Regulated Autophagy of Pancreatic Cancer Cells Through the AKT/Beclin 1 Signaling Pathway

Research has shown that autophagy is intertwined with the AKT/Beclin 1 signaling pathway [31]. To further explore the molecular mechanism by which COL11A1 regulates autophagy, we assessed the effect of COL11A1 on the AKT/Beclin 1 signaling pathway via western blotting, while additionally investigating its impact on phosphorylated mTOR (p-mTOR). The results showed that COL11A1 promoted the phosphorylation of AKT, mTOR, and Beclin 1 (Fig. 5a). Furthermore, western blotting analysis demonstrated that LY294002 attenuated the regulatory effect of COL11A1 on the expression levels of LC3, p62, and p-Beclin 1 (Fig. 5c). To further confirm that COL11A1 regulates autophagy via the AKT/Beclin 1 signaling pathway, we performed immunofluorescence experiments. The results demonstrated that LY294002 and siBeclin 1 attenuated the inhibitory effect of COL11A1 on LC3 expression (Fig. 5b). In addition, we assessed the effects of LY294002 and siBeclin 1 on COL11A1-induced changes in ROS and iron content via fluorescence-based assays. The results revealed that LY294002 and siBeclin 1 partially counteracted the regulatory effect of COL11A1 on ROS and iron content (Fig. 6a,b). Furthermore, the nude mouse tumor-bearing assay demonstrated that implantation of COL11A1-overexpressing PANC-1 cells significantly promoted *in vivo* tumor growth, whereas tumor volumes were markedly reduced following erastin or RAPA treatment (Fig. 6c). Collectively, these findings indicate that COL11A1 serves as a critical driver of pancreatic cancer progression, and its pro-tumorigenic function is closely associated with the ferroptosis and autophagy pathways. These data suggest that COL11A1 regulates the ferroptosis of pancreatic cancer cells through AKT/Beclin 1-dependent autophagy (Fig. 6d).

4. Discussion

PDAC is highly resistant to chemotherapy drugs [32, 33], with a 5-year survival rate consistently ranging between 5% and 10%. There is an urgent need to explore new pathological mechanisms and therapeutic targets to overcome current treatment bottlenecks.

A growing body of prior evidence has unequivocally demonstrated the specific upregulation of COL11A1 in pancreatic cancer tissues relative to adjacent normal tissues. These studies, encompassing mRNA expression profiling, comprehensive bioinformatics analyses, and histopathological examinations of clinical sections, consistently identify COL11A1 as a promising prognostic biomarker for poor outcomes in pancreatic cancer patients [34–36]. This study systematically delineates the pivotal role of COL11A1 in regulating ferroptosis in PDAC, and found three key findings outlined below: First, the cancer genome atlas (TCGA) database validation showed that COL11A1 is significantly overexpressed in PDAC tissues relative to adjacent non-

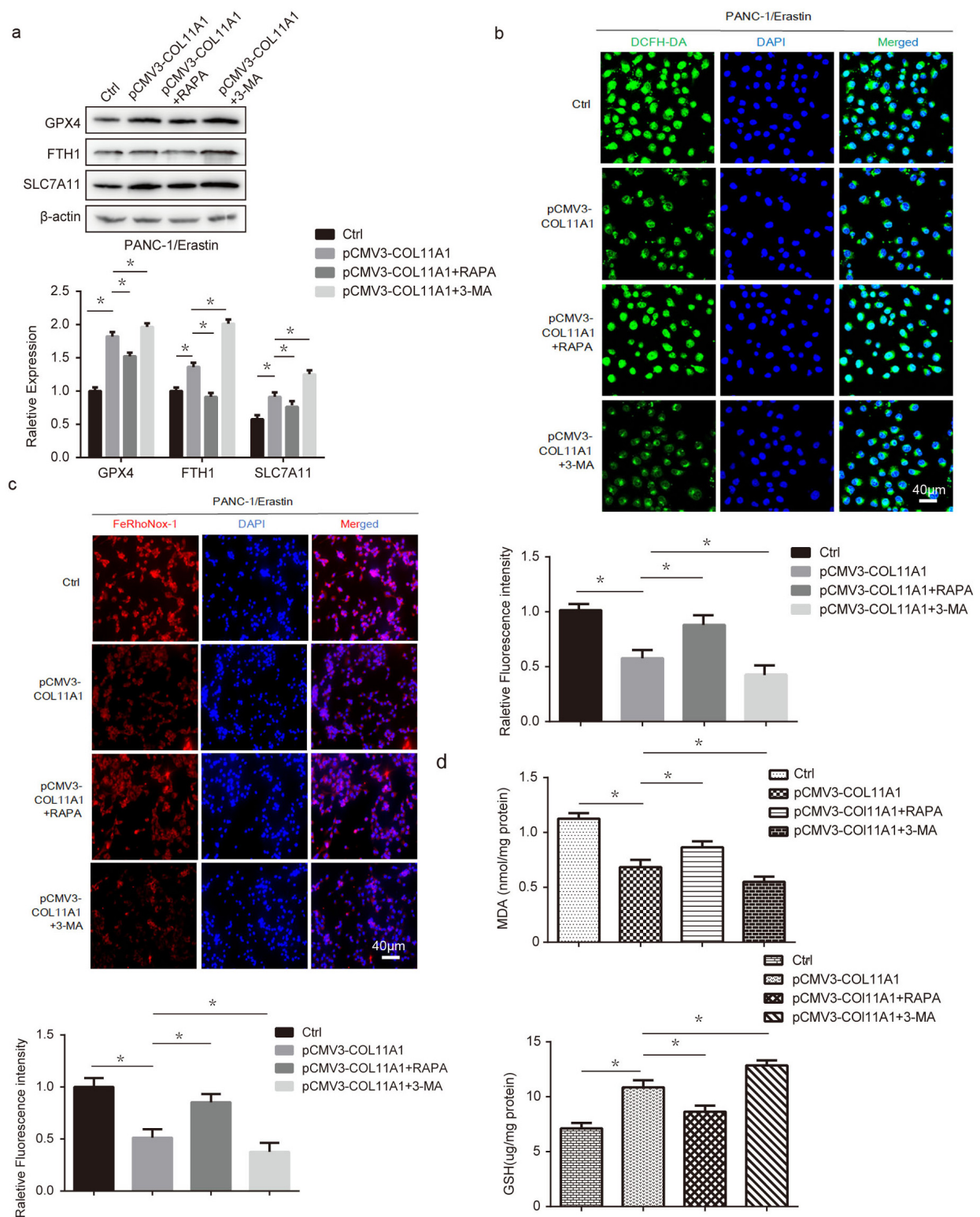


Fig. 4. COL11A1 regulated the ferroptosis process of pancreatic cancer cells through autophagy. (a) Western blotting was used to detect the expression levels of GPX4, SLC7A11, and FTH1 under treatment with erastin (10 μ M) and transfected pCMV3-COL11A1, pCMV3-COL11A1+RAPA, or pCMV3-COL11A1+3-MA. (b) Immunofluorescence was used to detect the expression of ROS by adding DCFH-DA under different treatments. Scale bar: 40 μ m. (c) Immunofluorescence was used to detect the expression level of iron visualized with the FeRhoNox-1 probe under different treatments. Scale bar: 40 μ m. (d) The GSH/MDA kit was used to detect the expression level of GSH/MDA under transfected pCMV3-COL11A1, pCMV3-COL11A1+RAPA, or pCMV3-COL11A1+3-MA. $n = 3$, $*p < 0.05$. 3-MA, 3-methyladenine.

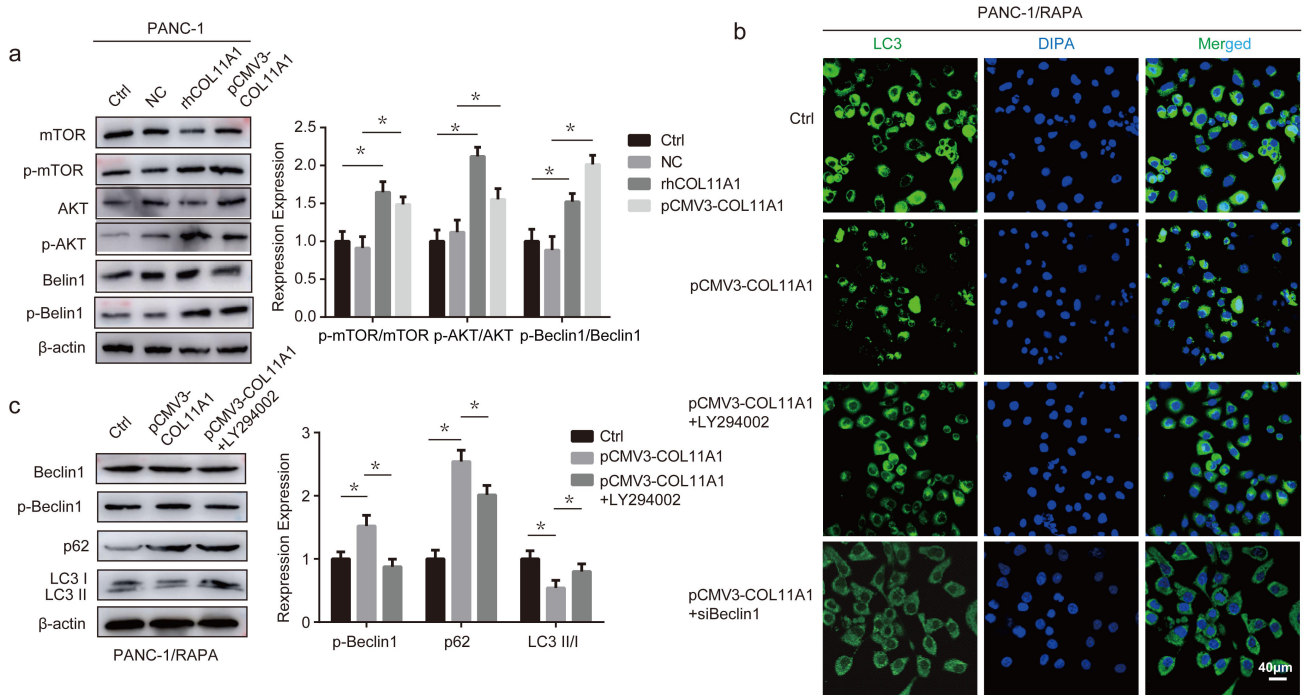


Fig. 5. COL11A1 regulated the autophagy of pancreatic cancer cells through the AKT/Beclin 1 signaling pathway. (a) Western blotting was used to detect the expression levels of AKT, p-AKT, mTOR, p-mTOR, Beclin 1, and p-Beclin 1 under treatment with pCMV3-COL11A1 or rhCOL11A1. (b) Immunofluorescence was used to detect the expression of LC3 under treatment with RAPA (100 nM) and transfected pCMV3-COL11A1, pCMV3-COL11A1+LY294002, or pCMV3-COL11A1+siBeclin 1. Scale bar: 40 μ m. (c) Western blotting was used to detect the expression levels of Beclin 1, p-Beclin 1, p62, and LC3II/I under treatment with RAPA (100 nM) and pCMV3-COL11A1 or pCMV3-COL11A1+LY294002. n = 3, * p < 0.05. p-mTOR, phosphorylated mTOR.

tumor tissues, and its expression negatively correlates with patient survival. Patients with high COL11A1 expression had a median survival time half that of the control group, indicating that COL11A1 may serve as an independent poor prognostic predictor for PDAC. Second, functional experiments verified that COL11A1 overexpression in PANC-1 pancreatic cancer cells reduced free iron content by 30–45% and MDA by 2–3 fold, while downregulating the key ferroptosis regulators GPX4 and SLC7A11. In summary, COL11A1 overexpression strongly antagonizes erastin-induced ferroptosis. Third, mechanistic investigations elucidated that COL11A1 activates the AKT signaling pathway, which promotes phosphorylation of its downstream molecule Beclin 1 and suppresses autophagic activity. Intervention using the AKT inhibitor LY294002 or Beclin 1 siRNA abrogated COL11A1-mediated ferroptosis inhibition, confirming that AKT/Beclin 1-dependent autophagy constitutes the core pathway through which COL11A1 regulates ferroptosis in PDAC.

Ferroptosis presents opportunities for mechanistic research due to its complex regulatory network, making it a promising area for potential therapeutic targeting in pancreatic cancer treatment. Previous studies have revealed that exosomes secreted by co-induced cancer-associated fibroblasts (CAFs) can suppress gemcitabine (GEM)-induced ferroptosis in PDAC cells [37]. Additionally, separate study

has established that CAFs themselves exert a protective effect on PDAC cells against ferroptosis induced by the small-molecule agents erastin and RSL3 [38]. However, the functional relevance of CAF-secreted extracellular matrix (ECM) components in regulating ferroptosis remains largely underexplored. Collagen, the predominant component of the ECM, is critically involved in remodeling the tumor microenvironment and regulating malignant biological behaviors of cancer cells. As a member of the collagen family, COL11A1 has been previously confirmed to be closely associated with the invasion, metastasis, and chemoresistance of pancreatic cancer [39], but no studies have explored its association with ferroptosis. In the present study, we demonstrate that COL11A1 inhibits the occurrence of ferroptosis in pancreatic cancer cells. Given that ferroptosis is closely associated with GEM resistance, targeting COL11A1 may offer a novel therapeutic avenue for addressing pancreatic cancer progression and chemoresistance.

The precise role autophagy plays in PDAC tumorigenesis is complicated by several conflicting studies that have shown that autophagy can lead to both promotion and inhibition of tumor development. A tumor-promoting mechanism of autophagy has been described in mice with heterozygous deletions of mammalian Beclin 1. Deletion of this key autophagy promoting enzyme results in the devel-

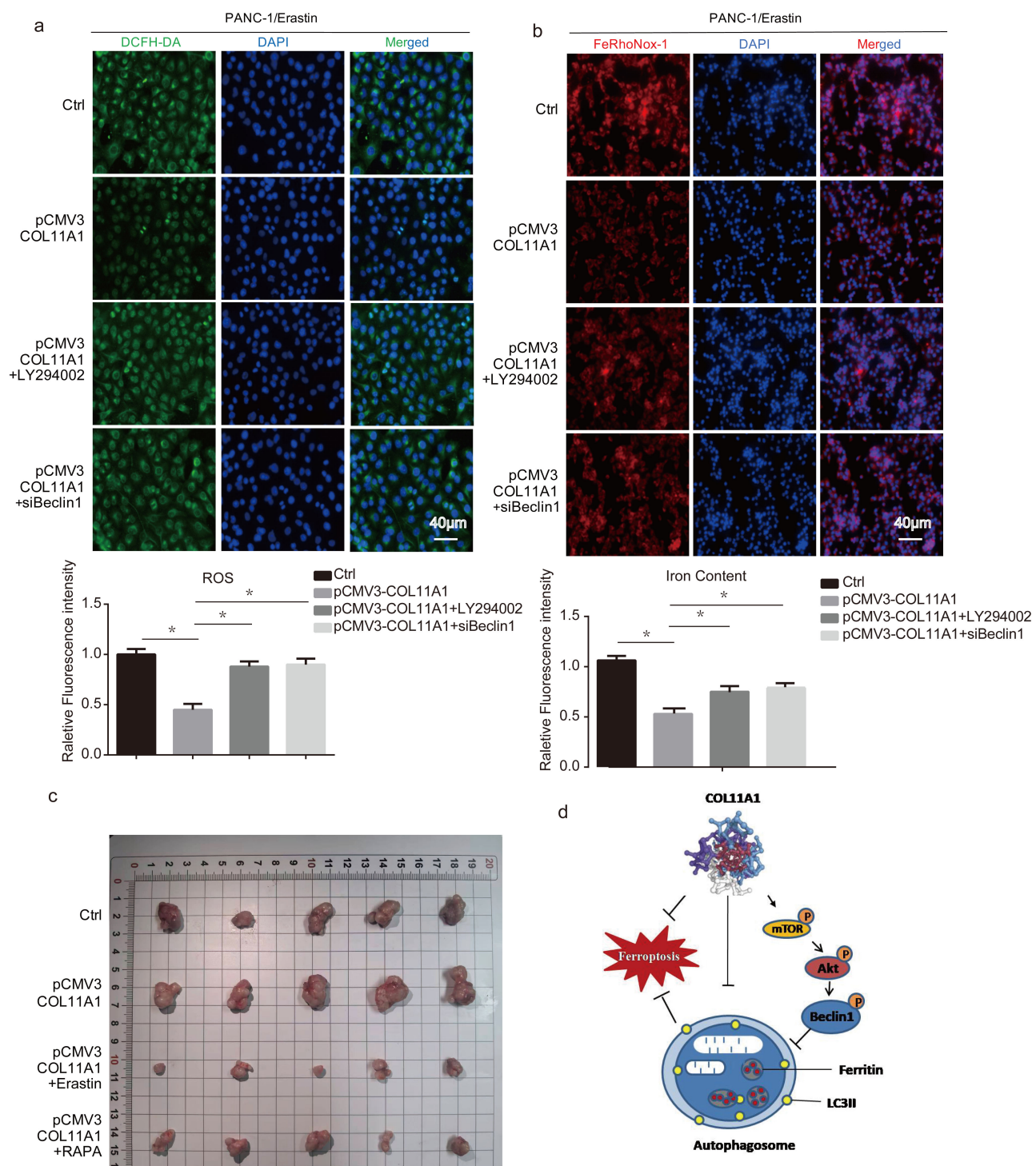


Fig. 6. COL11A1 regulated ferroptosis of pancreatic cancer cells through the AKT/Beclin 1 signaling pathway. (a) Immunofluorescence was used to detect the expression of ROS by adding DCFH-DA under treatment with erastin (10 µM) and pCMV3-COL11A1, pCMV3-COL11A1+LY294002, or pCMV3-COL11A1+siBeclin 1. Scale bar: 40 µm. (b) The results of immunofluorescence analysis of iron content in PANC-1 cells following different treatments are shown iron was visualized with FeRhoNox-1, and nuclei were stained with DAPI. Scale bar: 40 µm. (c) Wild-type PANC-1 cells and COL11A1 stably overexpressing PANC-1 cells were subcutaneously implanted into nude mice, respectively. In addition, two other groups were established, in which nude mice bearing COL11A1 stably overexpressing PANC-1 cell xenografts were treated with erastin (30 mg/kg) or RAPA (4 mg/kg), separately. The tumors were obtained at the end of the experiment. (d) Mechanism of COL11A inhibiting ferroptosis in pancreatic cancer by inhibiting AKT/Beclin 1 dependent autophagy. n = 3, *p < 0.05.

opment of malignant neoplasms in various organs in mice [40,41]. It has been suggested that autophagy is a relatively weak tumor suppressor yet at the same time it is necessary for the progression of benign tumors to malignancy [42]. There is also evidence suggesting that defects in autophagy lead to increased dysfunctional or damaged mitochondria in tumor cells and impaired tumorigenesis [43]. The “bidirectional regulatory” characteristic of autophagy in regulating ferroptosis has become a research hotspot [44,45]. This study found that COL11A1-mediated autophagy inhibition significantly reduced intracellular free iron accumulation and lipid peroxidation levels, which is consistent with the view that “a specific subtype of autophagy induces ferroptosis” [46]. From the perspective of signaling pathway crosstalk, the AKT/Beclin 1 pathway is a core node in autophagy regulation. Mechanistic studies revealed that COL11A1-activated AKT directly phosphorylates Beclin 1 at Ser-295, which suppresses autophagosome formation, thereby reducing ferritinophagy and the modulation of related processes, including iron metabolism, lipid peroxidation, and antioxidant activity. Ultimately, an inhibitory pathway of ferroptosis, namely, “COL11A1-AKT-Beclin 1-autophagy”, is formed. This finding refines the molecular mechanism of autophagy–ferroptosis crosstalk in pancreatic cancer and provides a new perspective for understanding how tumor microenvironment components regulate cell death modalities.

These findings are consistent with and further supported by multiple investigations in the field of pancreatic cancer. Regarding the oncogenic function of COL11A1, Yang *et al.* [47] demonstrated that COL11A1 promotes cancer metastasis via activation of the PI3K/AKT pathway. Building on this finding, the present study further confirms that the PI3K/AKT pathway can also mediate ferroptosis inhibition by regulating autophagy. These results collectively suggest that the AKT pathway acts as a critical signaling hub through which COL11A1 exerts its oncogenic effects. Regarding ferroptosis regulation, Zhu *et al.* [48] demonstrated that deletion of autophagy-related gene 5 potentiates the sensitivity of pancreatic cancer cells to ferroptosis inducers. This study established COL11A1 as an upstream regulator of this process, thereby enhancing the understanding of the upstream signaling network that links autophagy to ferroptosis. In addition, this study revealed that COL11A1’s regulation of ferroptosis depends on the AKT/Beclin 1 pathway, independent of the mitogen-activated protein kinase (MAPK) pathway. This finding complements the mechanism of MAPK regulating autophagy ferroptosis reported by Yang *et al.* [49], and highlights characteristics of parallel multiple pathways in ferroptosis regulation within pancreatic cancer.

The clinical significance of this study lies primarily in the development of biomarkers and optimization of treatment strategies. Specifically, for diagnosis and prognosis evaluation, the high expression of COL11A1 in pancreatic

cancer tissue and its association with a poor prognosis suggest its potential as a valuable diagnostic marker for pancreatic cancer. In terms of treatment strategy, this study confirmed that COL11A1 knockdown can significantly enhance the sensitivity of PANC-1 cells to erastin, which suggests that the combined treatment strategy of targeting COL11A1 using a ferroptosis inducer may become a new direction for the treatment of pancreatic cancer, especially for patients with drug-resistant cancer who have high expression of COL11A1.

5. Limitations

There are several limitations in the present study. First, the mechanism by which COL11A1 regulates ferroptosis via AKT/Beclin1-dependent autophagy was only validated in the PANC-1 model; its generalizability in other pancreatic cancer subtypes requires further investigation. Second, our animal study only evaluated tumor growth, without detecting the expression of ferroptosis and autophagy markers in tumor tissues, which limits the translational potential. Third, mechanistic assays relied solely on pharmacological inhibitors rather than genetic knockout, which may influence the interpretation of our results.

6. Conclusion

In summary, COL11A1 is highly expressed in pancreatic cancer and inhibits ferroptosis by activating AKT/Beclin 1-dependent autophagy. Its expression level is closely related to the poor prognosis of patients. This study not only identified a new function and molecular mechanism for COL11A1 in pancreatic cancer, but also offered a novel molecular target for prognosis evaluation and targeted treatment. The findings provide an important theoretical and experimental basis for overcoming the current limitations of pancreatic cancer treatment.

Availability of Data and Materials

The datasets used in this article are accessible from the corresponding author DDL upon request.

Author Contributions

HW designed the research study and responsible for cell experiments and molecular biology experiments, wrote the main manuscript text. SZ, LLD and JW processed experimental data and summarized experimental results. ZBY, JC and NG prepared figures. DDL guided experimental design and paper writing. All authors have participated sufficiently in the work and agreed to be accountable for all aspects of the work. All authors contributed to editorial changes in the manuscript. All authors read and approved the final manuscript.

Ethics Approval and Consent to Participate

This study was conducted in strict compliance with the Guidelines for the Ethical Review of Animal Welfare in Laboratory Animals. All experimental protocols involving animals were reviewed and approved by the Ethics Committee of Tianjin Institute of Medical & Pharmaceutical Sciences (Ethics Approval No. IMPS-EAEP-Z-KTSB-202312). Throughout the research process, we adhered rigorously to relevant national and international animal welfare regulations and guidelines to ensure the welfare and humane treatment of the laboratory animals.

Acknowledgment

Not applicable.

Funding

This research endeavor was funded by the Science and Technology Project of Tianjin Health Commission, grant number TJWJ2023QN096; National Natural Science Foundation of China, grant number 82304797.

Conflict of Interest

The authors declare no conflict of interest.

References

- [1] Siegel RL, Giaquinto AN, Jemal A. Cancer statistics, 2024. *CA: A Cancer Journal for Clinicians*. 2024; 74: 12–49. <https://doi.org/10.3322/caac.21820>.
- [2] Stoop TF, Javed AA, Oba A, Koerkamp BG, Seufferlein T, Wilmsink JW, *et al.* Pancreatic cancer. *Lancet*. 2025; 405: 1182–1202. [https://doi.org/10.1016/S0140-6736\(25\)00261-2](https://doi.org/10.1016/S0140-6736(25)00261-2).
- [3] Li Y, Lacerda DA, Warman ML, Beier DR, Yoshioka H, Nishimura Y, *et al.* A fibrillar collagen gene, *Col11a1*, is essential for skeletal morphogenesis. *Cell*. 1995; 80: 423–430. [https://doi.org/10.1016/0092-8674\(95\)90492-1](https://doi.org/10.1016/0092-8674(95)90492-1).
- [4] Vázquez-Villa F, García-Ocaña M, Galván JA, García-Martínez J, García-Pravia C, Menéndez-Rodríguez P, *et al.* COL11A1/(pro)collagen 11A1 expression is a remarkable biomarker of human invasive carcinoma-associated stromal cells and carcinoma progression. *Tumour Biology*. 2015; 36: 2213–2222. <https://doi.org/10.1007/s13277-015-3295-4>.
- [5] Karaglani M, Toumpoulis I, Goutas N, Poupouridou N, Vlachodimitropoulos D, Vasilaros S, *et al.* Development of novel real-time PCR methodology for quantification of COL11A1 mRNA variants and evaluation in breast cancer tissue specimens. *BMC Cancer*. 2015; 15: 694. <https://doi.org/10.1186/s12885-015-1725-8>.
- [6] Zheng X, Liu X, Zheng H, Wang H, Hong D. Integrated bioinformatics analysis identified COL11A1 as an immune infiltrates correlated prognosticator in pancreatic adenocarcinoma. *International Immunopharmacology*. 2021; 90: 106982. <https://doi.org/10.1016/j.intimp.2020.106982>.
- [7] Abbonante V, Malara A, Chrisam M, Metti S, Soprano P, Semplificini C, *et al.* Lack of COL6/collagen VI causes megakaryocyte dysfunction by impairing autophagy and inducing apoptosis. *Autophagy*. 2023; 19: 984–999. <https://doi.org/10.1080/15548627.2022.2100105>.
- [8] Nakamura T, Yamashita M, Ikegami K, Suzuki M, Yanagita M, Kitagaki J, *et al.* Autophagy facilitates type I collagen synthesis in periodontal ligament cells. *Scientific Reports*. 2021; 11: 1291. <https://doi.org/10.1038/s41598-020-80275-4>.
- [9] Zhou B, Liu J, Kang R, Klionsky DJ, Kroemer G, Tang D. Ferroptosis is a type of autophagy-dependent cell death. *Seminars in Cancer Biology*. 2020; 66: 89–100. <https://doi.org/10.1016/j.semcancer.2019.03.002>.
- [10] Zhu X, Li H, Xue T, Wang S, Zhu R, Luo J, *et al.* Mechanistic study on the role of multi-pathway autophagy in ovarian aging: literature review. *Apoptosis: an International Journal on Programmed Cell Death*. 2025; 30: 2694–2721. <https://doi.org/10.1007/s10495-025-02181-2>.
- [11] Gómez-Virgilio L, Silva-Lucero MDC, Flores-Morelos DS, Gallardo-Nieto J, Lopez-Toledo G, Abarca-Fernandez AM, *et al.* Autophagy: A Key Regulator of Homeostasis and Disease: An Overview of Molecular Mechanisms and Modulators. *Cells*. 2022; 11: 2262. <https://doi.org/10.3390/cells11152262>.
- [12] Deng Z, Sun M, Wu J, Fang H, Cai S, An S, *et al.* SIRT1 attenuates sepsis-induced acute kidney injury via Beclin 1 deacetylation-mediated autophagy activation. *Cell Death & Disease*. 2021; 12: 217. <https://doi.org/10.1038/s41419-021-03508-y>.
- [13] Dixon SJ, Lemberg KM, Lamprecht MR, Skouta R, Zaitsev EM, Gleason CE, *et al.* Ferroptosis: an iron-dependent form of nonapoptotic cell death. *Cell*. 2012; 149: 1060–1072. <https://doi.org/10.1016/j.cell.2012.03.042>.
- [14] Liu J, Liu Y, Wang Y, Li C, Xie Y, Klionsky D, *et al.* TMEM164 is a new determinant of autophagy-dependent ferroptosis. *Autophagy*. 2023; 19: 945–956. <https://doi.org/10.1080/15548627.2022.2111635>.
- [15] Kang R, Tang D. Autophagy and Ferroptosis - What's the Connection? *Current Pathobiology Reports*. 2017; 5: 153–159. <https://doi.org/10.1007/s40139-017-0139-5>.
- [16] Dixon SJ, Olzmann JA. The cell biology of ferroptosis. *Nature Reviews. Molecular Cell Biology*. 2024; 25: 424–442. <https://doi.org/10.1038/s41580-024-00703-5>.
- [17] Zhou Q, Meng Y, Li D, Yao L, Le J, Liu Y, *et al.* Ferroptosis in cancer: From molecular mechanisms to therapeutic strategies. *Signal Transduction and Targeted Therapy*. 2024; 9: 55. <https://doi.org/10.1038/s41392-024-01769-5>.
- [18] Zhang R, Chen J, Wang S, Zhang W, Zheng Q, Cai R. Ferroptosis in Cancer Progression. *Cells*. 2023; 12: 1820. <https://doi.org/10.3390/cells12141820>.
- [19] Li X, Si W, Zhang Y, Yang P, Ruan L, Ba H, *et al.* Alpha-Hereditin targets CAMKII/DRP1-Mediated mitochondrial fission to trigger ferroptosis in pancreatic ductal adenocarcinoma. *Phytomedicine*. 2025; 145: 157048. <https://doi.org/10.1016/j.phymed.2025.157048>.
- [20] Abdelmawgood IA, Hussien DM, Boushra MI. The role and interplay among Autophagy, Apoptosis, and ferroptosis in acute pancreatitis: mechanisms and therapeutic approaches. *Molecular Biology Reports*. 2025; 53: 208. <https://doi.org/10.1007/s11033-025-11319-z>.
- [21] Zhang Z, Lu M, Chen C, Tong X, Li Y, Yang K, *et al.* Holo-lactoferrin: the link between ferroptosis and radiotherapy in triple-negative breast cancer. *Theranostics*. 2021; 11: 3167–3182. <https://doi.org/10.7150/thno.52028>.
- [22] Niu B, Liao K, Zhou Y, Wen T, Quan G, Pan X, *et al.* Application of glutathione depletion in cancer therapy: Enhanced ROS-based therapy, ferroptosis, and chemotherapy. *Biomaterials*. 2021; 277: 121110. <https://doi.org/10.1016/j.biomaterials.2021.121110>.
- [23] Perera L, Brown SM, Silver BB, Tokar EJ, Sinha BK. Ferroptosis Inducers Erastin and RSL3 Enhance Adriamycin and Topotecan Sensitivity in ABCB1/ABCG2-Expressing Tumor Cells. *International Journal of Molecular Sciences*. 2025; 26: 635. <https://doi.org/10.3390/ijms26020635>.
- [24] Yang C, Dong Q, Bao H, Ge Y, Xu Z, Li J, *et al.* Ferroptosis:

New Strategies and Ideas for the Treatment of Pancreatic Ductal Adenocarcinoma. *Frontiers in bioscience (Landmark edition)*. 2024; 29: 45. <https://doi.org/10.31083/j.fbl2901045>.

- [25] Zhao Y, Hu X, Liu Y, Dong S, Wen Z, He W, *et al.* ROS signaling under metabolic stress: cross-talk between AMPK and AKT pathway. *Molecular Cancer*. 2017; 16: 79. <https://doi.org/10.1186/s12943-017-0648-1>.
- [26] Wei CC, Luo Z, Hogstrand C, Xu YH, Wu LX, Chen GH, *et al.* Zinc reduces hepatic lipid deposition and activates lipophagy via Zn²⁺/MTF-1/PPAR α and Ca²⁺/CaMKK β /AMPK pathways. *FASEB Journal*. 2018; fj201800463. <https://doi.org/10.1096/fj.201800463>.
- [27] Seo AY, Lau PW, Feliciano D, Sengupta P, Gros MAL, Cinquin B, *et al.* AMPK and vacuole-associated Atg14p orchestrate μ -lipophagy for energy production and long-term survival under glucose starvation. *eLife*. 2017; 6: e21690. <https://doi.org/10.7554/eLife.21690>.
- [28] Vereshchagina N, Wilson C. Cytoplasmic activated protein kinase Akt regulates lipid-droplet accumulation in *Drosophila* nurse cells. *Development*. 2006; 133: 4731–4735. <https://doi.org/10.1242/dev.02659>.
- [29] Cao J, Xu D, Wang D, Wu R, Zhang L, Zhu H, *et al.* ROS-driven Akt dephosphorylation at Ser-473 is involved in 4-HPR-mediated apoptosis in NB4 cells. *Free Radical Biology & Medicine*. 2009; 47: 536–547. <https://doi.org/10.1016/j.freeradbiomed.2009.05.024>.
- [30] Wang RC, Wei Y, An Z, Zou Z, Xiao G, Bhagat G, *et al.* Akt-mediated regulation of autophagy and tumorigenesis through Beclin 1 phosphorylation. *Science*. 2012; 338: 956–959. <https://doi.org/10.1126/science.1225967>.
- [31] Pu Z, Wu L, Guo Y, Li G, Xiang M, Liu L, *et al.* LncRNA MEG3 contributes to adenine-induced cytotoxicity in hepatoma HepG2 cells by downregulated ILF3 and autophagy inhibition via regulation PI3K-AKT-mTOR and beclin-1 signaling pathway. *Journal of Cellular Biochemistry*. 2019; 120: 18172–18185. <https://doi.org/10.1002/jcb.29123>.
- [32] Balachandran VP, Beatty GL, Dougan SK. Broadening the Impact of Immunotherapy to Pancreatic Cancer: Challenges and Opportunities. *Gastroenterology*. 2019; 156: 2056–2072. <https://doi.org/10.1053/j.gastro.2018.12.038>.
- [33] Binenbaum Y, Na'ara S, Gil Z. Gemcitabine resistance in pancreatic ductal adenocarcinoma. *Drug Resistance Updates*. 2015; 23: 55–68. <https://doi.org/10.1016/j.drug.2015.10.002>.
- [34] García-Pravia C, Galván JA, Gutiérrez-Corral N, Solar-García L, García-Pérez E, García-Ocaña M, *et al.* Overexpression of COL11A1 by cancer-associated fibroblasts: clinical relevance of a stromal marker in pancreatic cancer. *PLoS ONE*. 2013; 8: e78327. <https://doi.org/10.1371/journal.pone.0078327>.
- [35] Kleinert R, Prenzel K, Stoecklein N, Alakus H, Bollschweiler E, Hölscher A, *et al.* Gene Expression of Col11A1 Is a Marker Not only for Pancreas Carcinoma But also for Adenocarcinoma of the Papilla of Vater, Discriminating Between Carcinoma and Chronic Pancreatitis. *Anticancer Research*. 2015; 35: 6153–6158.
- [36] Sun D, Jin H, Zhang J, Tan X. Integrated whole genome microarray analysis and immunohistochemical assay identifies COL11A1, GJB2 and CTRL as predictive biomarkers for pancreatic cancer. *Cancer Cell International*. 2018; 18: 174. <https://doi.org/10.1186/s12935-018-0669-x>.
- [37] Qi R, Bai Y, Li K, Liu N, Xu Y, Dal E, *et al.* Cancer-associated fibroblasts suppress ferroptosis and induce gemcitabine resistance in pancreatic cancer cells by secreting exosome-derived ACSL4-targeting miRNAs. *Drug Resistance Updates*. 2023; 68: 100960. <https://doi.org/10.1016/j.drug.2023.100960>.
- [38] Zhu Y, Fang S, Fan B, Xu K, Xu L, Wang L, *et al.* Cancer-associated fibroblasts reprogram cysteine metabolism to increase tumor resistance to ferroptosis in pancreatic cancer. *Theranostics*. 2024; 14: 1683–1700. <https://doi.org/10.7150/thno.89805>.
- [39] Wang H, Zhou H, Ni H, Shen X. COL11A1-Driven Epithelial-Mesenchymal Transition and Stemness of Pancreatic Cancer Cells Induce Cell Migration and Invasion by Modulating the AKT/GSK-3 β /Snail Pathway. *Biomolecules*. 2022; 12: 391. <https://doi.org/10.3390/biom12030391>.
- [40] Qu X, Yu J, Bhagat G, Furuya N, Hibshoosh H, Troxel A, *et al.* Promotion of tumorigenesis by heterozygous disruption of the beclin 1 autophagy gene. *The Journal of Clinical Investigation*. 2003; 112: 1809–1820. <https://doi.org/10.1172/JCI20039>.
- [41] Yue Z, Jin S, Yang C, Levine AJ, Heintz N. Beclin 1, an autophagy gene essential for early embryonic development, is a haploinsufficient tumor suppressor. *Proceedings of the National Academy of Sciences of the United States of America*. 2003; 100: 15077–15082. <https://doi.org/10.1073/pnas.2436255100>.
- [42] Takamura A, Komatsu M, Hara T, Sakamoto A, Kishi C, Waguri S, *et al.* Autophagy-deficient mice develop multiple liver tumors. *Genes & Development*. 2011; 25: 795–800. <https://doi.org/10.1101/gad.2016211>.
- [43] White E. The role for autophagy in cancer. *The Journal of Clinical Investigation*. 2015; 125: 42–46. <https://doi.org/10.1172/JC173941>.
- [44] Chen F, Cai X, Kang R, Liu J, Tang D. Autophagy-Dependent Ferroptosis in Cancer. *Antioxidants & Redox Signaling*. 2023; 39: 79–101. <https://doi.org/10.1089/ars.2022.0202>.
- [45] Lv X, Wang B, Dong M, Wang W, Tang W, Qin J, *et al.* The crosstalk between ferroptosis and autophagy in cancer. *Autoimmunity*. 2023; 56: 2289362. <https://doi.org/10.1080/08916934.2023.2289362>.
- [46] Huang F, Cai Y, Ren M, Zhang X, Fu Y, Cheng R, *et al.* Salidroside sensitizes Triple-negative breast cancer to ferroptosis by SCD1-mediated lipogenesis and NCOA4-mediated ferritinophagy. *Journal of Advanced Research*. 2025; 74: 589–607. <https://doi.org/10.1016/j.jare.2024.09.027>.
- [47] Yang SY, Zhu LH, Yang R, Liao TT, Hu XW. COL11A1 regulates PI3K/Akt/GSK-3 β pathway and promotes human lung adenocarcinoma primary cell migration and invasion. *ZhonghuaJie He He Hu Xi Za Zhi*. 2023; 46: 580–586. <https://doi.org/10.3760/cma.j.cn112147-20220712-00596>. (In Chinese)
- [48] Zhu H, Zhong Y, Chen R, Wang L, Li Y, Jian Z, *et al.* ATG5 Knockdown Attenuates Ischemia-Reperfusion Injury by Reducing Excessive Autophagy-Induced Ferroptosis. *Translational Stroke Research*. 2024; 15: 153–164. <https://doi.org/10.1007/s12975-022-01118-0>.
- [49] Yang MH, Baek SH, Jung YY, Um JY, Ahn KS. Activation of autophagy, paraptosis, and ferroptosis by micheliolide through modulation of the MAPK signaling pathway in pancreatic and colon tumor cells. *Pathology, Research and Practice*. 2024; 263: 155654. <https://doi.org/10.1016/j.prp.2024.155654>.